

Oblique Flame-Wall Interaction in Premixed Turbulent Combustion Under Isothermal and Adiabatic Wall Boundary Conditions

Umair Ahmed, Nilanjan Chakraborty

School of Engineering, Newcastle University, Newcastle-Upon-Tyne, NE1 7RU, United Kingdom

Markus Klein

Bundeswehr University Munich, Werner Heisenberg Weg 39, D-85577 Neubiberg, Germany

1 Introduction

Flame-wall interaction (FWI) occurs in many flows of engineering interest (e.g., Spark Ignition (SI) engines and gas turbines), and modelling these events remains challenging. The turbulence structure is altered by the walls, and the interaction of flame elements with walls leads to modifications of the underlying combustion process [1]. Spatial and temporal fluctuations of wall temperature induce thermal stresses and strongly affect combustor lifetimes. Furthermore, typical reaction rate closures of turbulent premixed combustion such as the flame-surface density [2] and scalar dissipation rate [3] based models do not account for the effects of boundary layer and different wall boundary conditions in the modelling approach. Therefore, fundamental physical understanding of premixed FWI is necessary for developing a new generation of computationally efficient reaction rate closures which play an important role in the optimisation and design of environment friendly devices for power generation and automotive engines. In this work oblique flame-wall interaction has been investigated for adiabatic and isothermal wall conditions, by performing Direct Numerical Simulation (DNS) of V-flames in a fully developed channel flow configuration. This configuration is representative of bluff body stabilised flames in gas turbine engines and industrial furnaces. The quantities requiring closures in the Reynolds Averaged Navier-Stokes (RANS) framework i.e. turbulent kinetic energy \tilde{k} , turbulent dissipation $\tilde{\epsilon}$, flame surface density Σ and scalar dissipation rate $\tilde{\epsilon}_c$ have been evaluated from the DNS data, so that the statistical behaviours of these quantities can be compared for adiabatic and isothermal wall boundary conditions.

2 Direct Numerical Simulation Data

A well-known three-dimensional compressible DNS code SENGGA [5] has been used to simulate the oblique flame-wall interaction of a V-flame with inert isotherothermal and adiabatic walls in a fully developed turbulent channel flow. The code employs high-order finite-difference (10th order for internal points and gradually decreasing to 2nd order at the non-periodic boundaries) and Runge-Kutta (3rd order explicit) schemes

for spatial differentiation and time advancement, respectively. It solves the governing equations of mass, momentum, energy, and species mass fractions in a non-dimensional form. A single step irreversible chemical mechanism ($Fuel + s Oxidiser \rightarrow (1 + s)Products$) (where s is oxidiser-fuel ratio) is used for the purpose of computational economy. The thermo-physical properties such as dynamic viscosity, thermal conductivity, and density-weighted mass diffusivity are taken to be constant and independent of temperature. Standard values of the Zeldovich number $\beta_z = T_a(T_{ad} - T_R/T_{ad}^2)$ (where T_a is the activation temperature, T_R is the reactant temperature and T_{ad} is the adiabatic flame temperature), Prandtl number Pr , and ratio of specific heats γ (i.e., $\beta_z = 6.0$, $Pr = 0.7$, and $\gamma = 1.4$ are used where the Lewis numbers of all the species are taken to be unity. The heat release parameter $\tau = (T_{ad} - T_R)/T_R$ is taken to be 2.3 for the V-flames.

An auxiliary DNS of inert fully developed turbulent-plane channel flow driven by a stream wise constant pressure gradient is used to generate the initial conditions and the inflow data for the reacting flow simulation. It can be shown by an overall momentum balance that the pressure gradient is directly related to the averaged shear stress (ρu_τ^2) as $-\partial p/\partial x = \rho u_\tau^2/h$, where $u_\tau = \sqrt{\tau_w/\rho}$ is the friction velocity, $\tau_w = \mu \partial u/\partial y|_{y=0}$ is the wall shear stress, h is the channel half height and μ is the dynamic viscosity of the fluid. The bulk Reynolds number $Re_b = \rho u_b h/\mu$ for this simulation is 3285, where $u_b = 1/2h \int_0^{2h} u dy$, and the wall friction based Reynolds number $Re_\tau = \rho u_\tau h/\mu$ is 110. It is ensured that the non-dimensional distance to the wall $y^+ = \rho u_\tau y/\mu$, where y is the distance from the wall, is below $y^+ = 0.6$ and the region $y^+ < 1$ has at least two grid points to ensure appropriate resolution of the boundary layer as recommended by Moser et al. [8]. The domain size for this channel is $10.72h \times 2h \times 4h$ and is discretised on $1920 \times 360 \times 720$ equidistant grid points.

Two different V-flame simulations have been performed, one with adiabatic walls (case-A) and the other with isothermal walls (case-B). The V-flame simulations are performed by placing a flame holder in a fully developed channel flow at $y^+ = 55$ (i.e. $y = 0.25h$ from the bottom wall), which ensures that the flame interacts with the bottom wall at a reasonable distance and also that the viscous boundary layer is not affected by the flame holder and any effects seen in the boundary layer downstream of the flame holder are due to the effects of thermal expansion. At the flame holder, the species, temperature and velocity distributions were imposed using a presumed Gaussian function following Dunstan et al. [6]. The formation of boundary layer on the flame holder and the effects of shear generated turbulence due to the flame holder are not considered in this analysis. The velocity fluctuations introduced at the inflow of the reacting channel are obtained by temporal sampling of the "temporally evolving turbulence" at a fixed stream wise location in the auxiliary non-reacting simulation. Note that the time step chosen for the non-reacting simulation, while the data is being sampled, is the same as that of the reacting flow simulation. The set-up for the V-flame calculation is shown in Fig. 1, where the progress variable is defined in terms of the fuel mass fraction. Navier-Stokes characteristic boundary conditions (NSCBC) [7] are used in the x and y directions. The boundary conditions are inflow at $x = 0$ and partially non-reflecting outflow at $x = 10.72h$ planes; no slip conditions are imposed for velocity at the walls at $y = 0$ and $y = 2h$, while the temperature is imposed using adiabatic conditions (i.e. $\partial T/\partial y|_{y=0}$ or $y=2h} = 0$) in case-A and isothermal (i.e. $T_{wall} = T_R$) conditions are used for case-B. The boundaries in z direction are treated as periodic. The walls are assumed to be inert and impermeable, hence normal mass flux for all species is set to zero at the walls. These simulations are representative of stoichiometric methane-air mixture at unity Lewis number under atmospheric conditions. The flame speed to friction velocity ratio $S_L/u_\tau = 0.7$ and the laminar flame thermal thickness δ_{th} is resolved in approximately 8 grid points, where $\delta_{th} = (T_{ad} - T_R)/max|\nabla T|_L$ with the subscript L representing the laminar flame quantities. The simulations have been performed for approximately 2 flow through times and the data has been sampled after 1 flow through time once the initial transience have decayed.

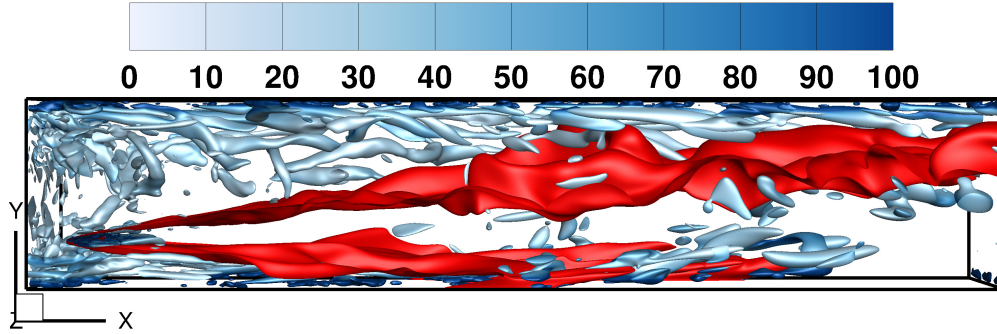


Figure 1: Adiabatic V-flame simulation. The iso-surface coloured in red represents $c = 0.5$. The iso-surfaces coloured in blue represent the Q -criterion coloured by vorticity magnitude.

In the post-processing of the DNS data, the Reynolds averaged quantities (denoted by $\bar{\lambda}$), Favre averaged quantities (denoted by $\tilde{\lambda} = \overline{\rho\lambda}/\bar{\rho}$), and Favre fluctuations (denoted by $\lambda'' = \lambda - \tilde{\lambda}$) have been time averaged and then space averaged in the periodic (z) direction at a given x location, where λ refers to a general quantity.

3 Results and Discussion

The non-reacting auxiliary channel flow simulation has been compared with the results of Tsukahara et al [9]¹ at $Re_\tau = 110$ and an excellent agreement has been obtained. Figure 2 shows the mean progress variable for the two V-flame cases investigated. It can be seen that the flame interacts with the wall earlier in the case of adiabatic wall conditions while the flame tends to interact with the wall further downstream in the case of isothermal wall conditions. This behaviour of the flame is expected due to the differences in the reaction rate at the wall in the two cases investigated. Some of these features have been explored further by interrogating the mean quantities including turbulence kinetic energy $\tilde{k} = 0.5\overline{u_i''u_i''}$, turbulence dissipation $\tilde{\epsilon} = \overline{\mu\partial u_i''/\partial x_j\partial u_i''/\partial x_j}/\bar{\rho}$, mean reaction rate of the progress variable $\overline{\omega_c}$, flame surface density $\Sigma = |\nabla c|$ and the scalar dissipation rate of the progress variable $\tilde{\epsilon}_c = \overline{\rho\alpha_c\partial c''/\partial x_i\partial c''/\partial x_i}/\bar{\rho}$, where α_c is the diffusivity of the progress variable. The data has been extracted at three sampling locations labelled as a, b and c in Fig. 2.

The behaviours of the mean values of density, stream wise velocity, progress variable and non-dimensional temperature ($T = (\hat{T} - T_R)/(T_{ad} - T_R)$, where \hat{T} is the local temperature at a given point) are shown in Fig. 3 for the two cases at location b. Note that some differences for the mean quantities are observed between different sampling locations but the results at location b are presented here for the sake of conciseness. It can be seen in Fig. 3 that the behaviours of mean values of density, progress variable and temperature are significantly different near the bottom wall region ($0.25 \geq y/h \geq 0$) for the two cases, while the mean stream wise velocity is unaffected by the change in the wall boundary condition. Note that the temperature at the bottom wall does not reach the adiabatic flame temperature and decoupling between the progress variable and temperature can be observed for case-B. This behaviour is expected in case-B due to the heat loss at the isothermal walls. In order to investigate the near wall region for both cases the behaviour of the mean values of turbulence kinetic energy, turbulence dissipation and mean reaction rate is plotted in Fig. 4. It can be seen that the behaviour of \tilde{k} is similar for the two cases, whereas the behaviour of $\tilde{\epsilon}$ is

¹Database available online at: <https://www.rs.tus.ac.jp/t2lab/db/>

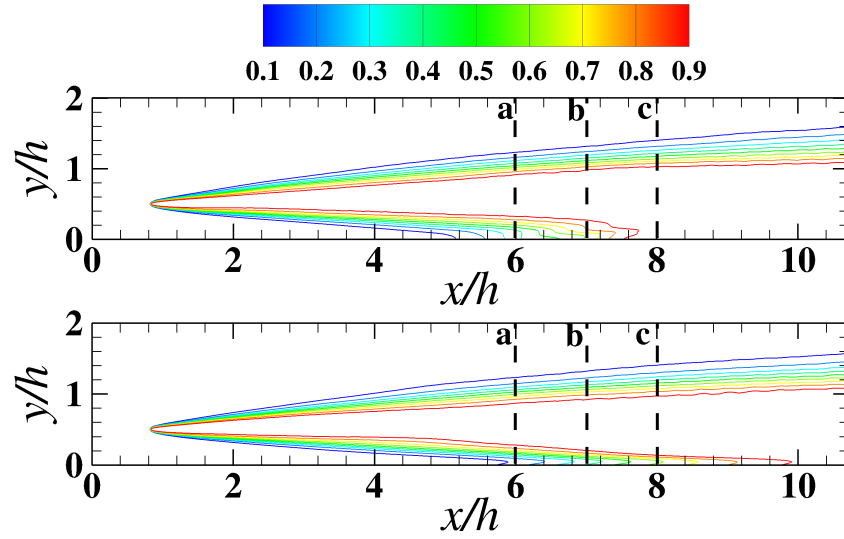


Figure 2: Contours of the progress variable c for the V-flames under adiabatic (top) and isothermal (bottom) wall conditions.

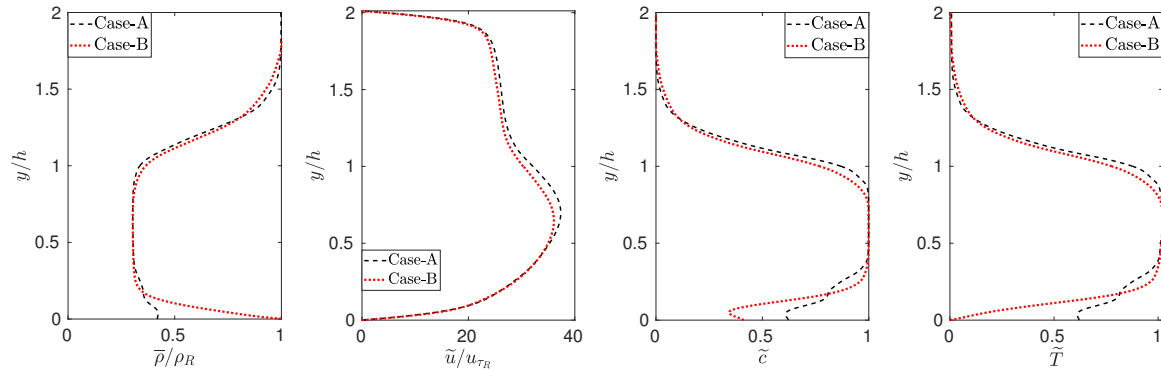


Figure 3: Mean profiles of density, stream wise velocity, progress variable and temperature.

different at the walls. In case-A the $\tilde{\epsilon}$ is higher at the bottom wall when compared with case-B. This is due to the variation of density at the bottom wall (see Fig. 3) resulting from the different thermal wall boundary condition used in the two cases. The mean reaction rate away from the bottom wall is almost identical in the two cases as shown in Fig. 4, but a significant difference can be observed between the two cases near the bottom wall. In case-A a significant reduction in the mean reaction rate can be seen near the bottom wall but the reaction rate remains non-zero while in case-B the reaction rate goes to zero at the wall. This implies that the fluid mechanical effects lead to the reduction of the reaction rate in case-A (i.e. quenching of the flame due to high straining), whereas in case-B the flame quenches due to the low temperature at the bottom wall. Figure 5 shows the mean values of progress variable, temperature, turbulence dissipation and the reaction rate on a logarithmic scale near the bottom wall region of the two flames. It can be observed that the mean reaction rate in case-A decreases in the regions of high turbulence dissipation which represents regions of high straining. Quenching due to high strain rate has been experimentally observed by Bradley et al. [4]. The aerodynamic quenching in case-A occurs due to the low ratio of laminar flame speed to the

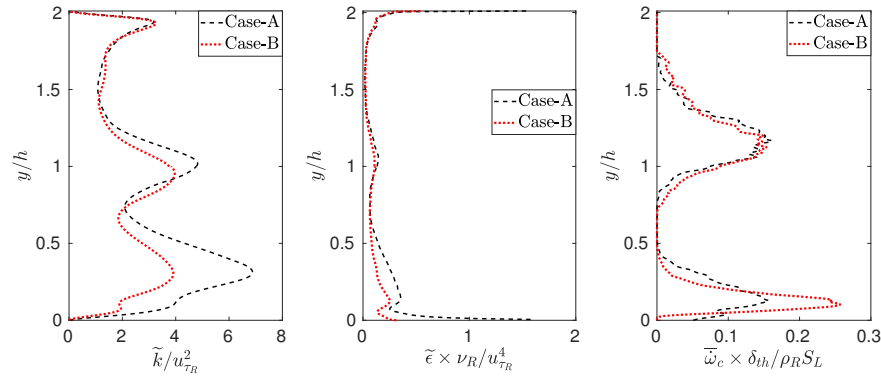


Figure 4: Mean profiles of turbulence kinetic energy, turbulence dissipation and reaction.

friction velocity S_L/u_τ .

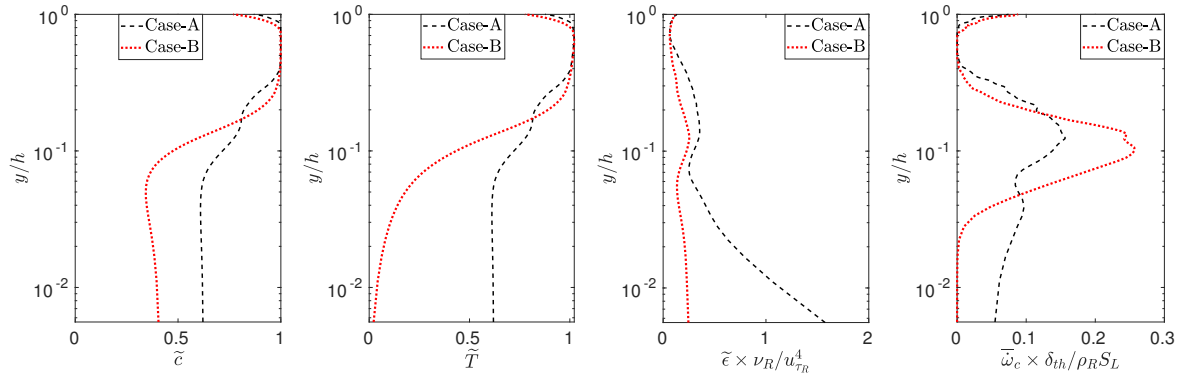


Figure 5: Mean profiles of progress variable, temperature, turbulence dissipation and reaction rate plotted on a logarithmic scale in the near wall region.

The behaviours of the mean flame surface density and scalar dissipation rate is shown in Fig. 6. In both cases Σ and $\tilde{\epsilon}_c$ decrease at the bottom wall, but higher levels of mean scalar dissipation rate can be seen at the wall for case-A when compared with that of case-B. Note that the reaction rate closures based on mean flame surface density ($\bar{\omega}_c = \rho_R S_L \Sigma$) and scalar dissipation rate ($\bar{\omega}_c = 2\bar{\rho}\tilde{\epsilon}_c/(2C_m - 1)$, where $C_m = 0.78$ for the thermochemistry considered in this work) are able to capture the reaction rate trends in case-A but predict a non-zero reaction rate at the wall for case-B. These closures need to be modified for isothermal conditions considered in this work, as the existing closures in the literature lead to high reaction rate predictions in the near wall regions due to high Σ and $\tilde{\epsilon}_c$ values near the bottom wall as shown in Fig. 6.

4 Conclusions

Two different V-flame simulations in a fully developed turbulent channel flow have been performed at $Re_\tau = 110$ under adiabatic and isothermal wall conditions. Mean quantities such as turbulence kinetic energy, and its dissipation rate, mean reaction rate, flame surface density and scalar dissipation rate have been investigated. It is found that the location of the oblique flame-wall interaction is slightly altered by the choice of the wall boundary condition. Variations in the mean values of progress variable, temperature, density and reaction rate have been observed for the two cases. Some features of aerodynamic quenching

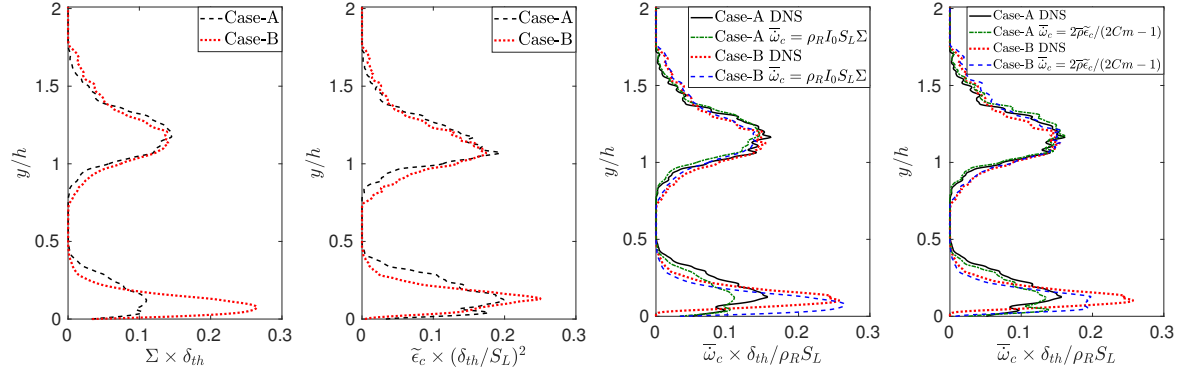


Figure 6: Mean profiles of flame surface density, scalar dissipation rate and the mean reaction rates evaluated from Σ and $\tilde{\epsilon}_c$.

have been observed for the V-flame under adiabatic conditions, which occurs due to the low S_L/u_τ ratio considered in this work. Furthermore, mean flame surface density and scalar dissipation rate statistics have also been calculated and it is found that the reaction rate closures based on these quantities need to be modified for the conditions considered in this work.

Acknowledgments

The authors are grateful to EPSRC (EP/P022286/1) for the financial support. The computational support was provided by ARCHER (EP/K025163/1) and the HPC facility at Newcastle University (Rocket).

References

- [1] Alshaalan, T.M., Rutland, C.J. (1998). Turbulence, scalar transport, and reaction rates in flame-wall interaction, Proc. Combust. Inst. 27:793.
- [2] Cant, R.S., et al. (1991) Modelling of flamelet surface-to-volume ratio in turbulent premixed combustion, Proc. Combust. Inst. 23, 809-815.
- [3] Bray, K.N.C. (1979). The interaction between turbulence and combustion. Proc. Combust. Inst. 17(1), 223-233.
- [4] Bradley, D., et al. (1998). The modeling of aerodynamic strain rate and flame curvature effects in premixed turbulent combustion. Proc. Combust. Inst. 27, 849-856.
- [5] Jenkins, K., Cant, R. (1999). Direct numerical simulation of turbulent flame kernels. In: Knight, D., Sakell, L.(eds.)Recent Advances in DNS and LES: Proceedings of the Second AFOSR Conference, Rutgers - The State University of New Jersey, New Brunswick, USA, pp. 191202. Kluwer, Dordrecht
- [6] Dunstan, T.D., et al. (2011). Geometrical properties and turbulent flame speed measurements in stationary premixed V-flames using Direct Numerical Simulation. Flow Turb. Combust., 87: 237-259.
- [7] Yoo, C.S., Im, H.G., (2007). Characteristic boundary conditions for simulations of compressible reacting flows with multi-dimensional, viscous and reaction effects. Combust. Theory Model. 11(2), 259-286
- [8] Moser, R. D., et al. (1999). Direct numerical simulation of turbulent channel flow up to $Re_\tau = 590$. Phys. Fluids, 11(4):943.
- [9] Tsukahara, T., et al (2005). 4th Int. Symp. on Turbulence and Shear Flow Phenomena, Williamsburg, VA, USA, 27-29, pp. 935-940